www.ietdl.org

Published in IET Microwaves, Antennas & Propagation
Received on 3rd December 2010
Revised on 11th January 2011
doi: 10.1049/iet-map.2010.0580

ISSN 1751-8725

Calibrated non-linear vector network measurement without using a multi-harmonic generator

J. Hu K.G. Gard M.B. Steer

Department of Electrical and Computer Engineering, North Carolina State University, Raleigh, NC 27695-7914, USA
E-mail: jhu@ncsu.edu

Abstract: The current generation of non-linear vector network analysers (NVNA) relies on a multi-harmonic generator to establish an absolute phase reference. Such a reference may not be readily available or, more importantly, may impose limitations on tone spacing in multi-tone testing for one type of NVNA based on a four-port VNA. The latter is a severe limitation when characterising memory behaviour in RF non-linear circuits. Here a hybrid NVNA is proposed that combines a sampling oscilloscope, a four-port VNA and phase-locked signal generators. A signal generator, phase locked to generators that are combined as the multi-tone excitation, provides the relative phase reference during swept power measurements using the VNA. The high dynamic range VNA-based measurements are corrected in absolute phase using the oscilloscope-based NVNA measurement at a specific power level. The hybrid NVNA has high dynamic range and the lower bound on tone spacing is determined by the memory depth of the oscilloscope, the windowing effect of the VNA receivers and the phase noise of the multi-tone sources. At 2 GHz, the hybrid NVNA has a dynamic range of 40 dB at 200 Hz tone spacing for a two-tone signal, increasing to more than 80 dB for tone spacings of 200 kHz and greater.

1 Introduction

Non-linear microwave and RF circuits and systems are experimentally characterised by exciting them using a multi-tone signal, generally a two-tone, and measuring the amplitudes and phases of individual spectral components of port voltages and currents. The type of instrument that makes these measurements is called a non-linear vector network analyser (NVNA). The equivalent-time sampling oscilloscope-based NVNA [1] is wideband (e.g. 20 GHz), but has a moderate 60 dB spurious free dynamic range (SFDR) and slow data acquisition. The sub-sampling mixer-based NVNA [1] is also wideband with a moderate 60 dB SFDR. For both of these NVNAs tone spacing is arbitrary. The four-port VNA-based NVNA [2] has a super-heterodyne architecture, is wideband and has a high SFDR of 85 dB. However, the minimum tone spacing is quite large.

Each of the above NVNAs is wideband and can be vector corrected to a measurement plane and power calibrated. A major difference is the absolute phase calibration which removes the receiver and interconnect phase dispersion when measuring a broad range of spectral components. Using a two-tone test signal, for example, this establishes the phase at the reference planes for each of the test tones and also for the intermodulation (IM) frequencies with respect to the phases of the test tones. For the oscilloscope-based NVNA and the sub-sampling mixer-based NVNA, absolute phase calibration uses a multi-harmonic generator, which is characterised by a nose-to-nose calibrated sampling oscilloscope. Then the multi-harmonic generator serves as a phase transfer standard to determine the receiver phase dispersion across the broad range of spectral components being measured. However, the broadband nature of the receivers' limits the dynamic range of both of these NVNAs.

The heterodyne receivers of a four-port VNA-based NVNA achieve high dynamic range because of their narrow instantaneous bandwidth (typically 250 kHz). However, each spectral component must be sequentially sampled one at a time and absolute phase calibration is established using a reference receiver (synchronised with the other receivers) to measure the output of a multi-harmonic generator at the same frequency as that of the DUT's spectral component to be measured. Thus, the reference receiver serves to transfer the phase reference from the multi-harmonic generator to the spectral component being characterised. This effectively relates the phase of sequentially sampled spectral components. While this method creates a broadband NVNA from an instrument with narrowband receivers, it is also the cause of the limitation on tone spacings. Typically, a multi-harmonic generator is driven at a low frequency fundamental, the grid frequency, f_{grid}, to produce harmonic tones on a grid, that is, at nf_{grid}, reducing in amplitude as n increases. This grid defines the frequencies of the two-tone signal with the minimum tone spacing being f_{grid}. The need for a harmonic reference tone to have an acceptable signal-to-noise ratio (SNR) at the two-tone signal frequencies establishes the minimum f_{grid}, that is, the minimum tone spacing. For example, the VNA-based NVNA in [2] has a minimum f_{grid} of 1.242 MHz for a two-tone test signal

© The Institution of Engineering and Technology 2011

centred at 3.01185 GHz; and a commercially available NVNA of this type has a minimum tone spacing of 10 MHz.

The NVNA introduced in this paper is a hybrid of the heterodyne-based and oscilloscope-based NVNAs. The architecture of the hybrid NVNA is presented in Section 2. The hybrid NVNA achieves high SFDR while also eliminating the tone-spacing limitation. A typical measurement characterises the amplitude and phase of an IM tone as the power of a two-tone input signal is swept. At the higher end of the power sweep, sampling oscilloscope measurements provide absolute phase measurements following nose-to-nose calibration of the sampling oscilloscope [3] to establish an absolute phase reference. However, the dynamic range of the oscilloscope-based measurements is limited. At the lower end of the power sweep the VNA-based measurements (having high dynamic range) provide relative phase measurements that are converted to absolute phase measurements by performing VNA-based and oscilloscope-based measurements at the same power level. The phase-locked (specifically not frequency-locked) reference oscillator, set to the frequency of the tone being characterised and measured by the reference receiver in the VNA, provides the phase transfer mechanism for each spectral component during a power sweep. Since the reference oscillator can be tuned with a finer frequency resolution, typically of the order of 1 Hz, there is effectively no tone-spacing limitation.

Section 3 uses the hybrid NVNA in the non-linear characterisation of a power amplifier that has long-term memory effects. The characteristics and limitations of the hybrid NVNA are discussed in Section 4. The demonstrated dynamic range is 80 dB for tone spacings of 200 kHz and greater. This reduces monotonically to 40 dB for tone spacings of 200 Hz, where the limitation derives from the spectral leakage associated with the FFT window used in the heterodyne VNA receivers and from the phase noise of the test signal.

2 Hybrid NVNA

The architecture of the hybrid NVNA is shown in Fig. 1*a*. Noticeably absent is a multi-harmonic generator to establish an absolute phase reference. The four-port VNA portion is used to make sequential measurements at each spectral component during a two-tone power sweep. The output of the top two of the RF generators are combined as the two-tone test signal. The third generator provides the relative phase reference for the spectral component being measured. The output of this reference RF generator is measured by the VNA reference receiver. The load connected to the reference RF generator is required, because the signal split from that branch will be used later in the phase calibration measurement which is shown in Fig. 1*b*.

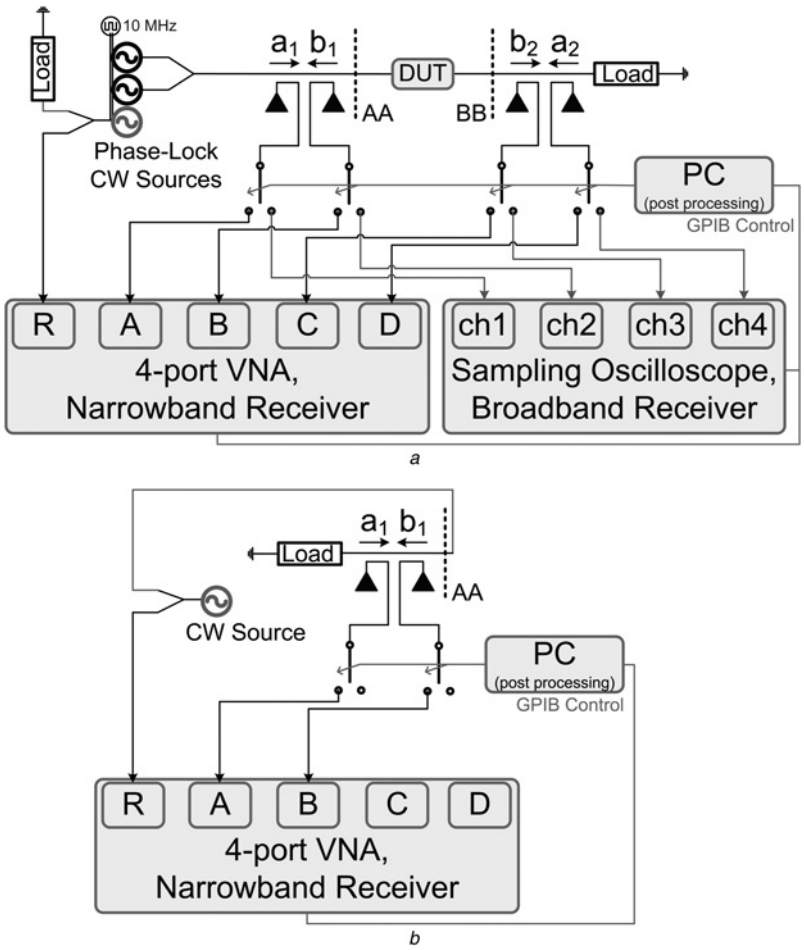

Fig. 1 *Connection diagrams of the proposed hybrid NVNA*

a For DUT measurement
b For phase calibration measurement
Proposed hybrid NVNA system combines a sampling oscilloscope-based NVNA and a four-port VNA-based NVNA, with phase-locked signal generators for multi-tone testing

© The Institution of Engineering and Technology 2011

In the measurement performed by the VNA portion of the hybrid NVNA, the phase-locked sources, together with the phase-synchronous VNA receivers, serve as the phase transfer mechanism that relates the sequential measurements during a power sweep at a particular spectral component. As such, the RF generators and the receiver channels must be phase synchronous. A common reference is used to phase-lock (not frequency-lock) three RF generators, although the relative phases of the generators are random. If the frequency of one of the RF generators is changed, these relative phases will be randomised but the phase relationship is fixed if only the signal level changes. The phase-locked sources and frequency-locked sources differ in the time duration of their true phase-lock. In typical frequency-locked sources, the synthesiser architecture uses dithering to reduce the level of spurious tones. As a result, the random phase variations of the independent fractional synthesisers only have a particular time-varying phase relationship on average. This has been empirically verified by comparing the phases measured by two receiver channels of the VNA. The outputs of two phase-locked sources such as the Marconi 2024 are phase-synchronous for a long duration (typically for several hours), while the outputs of two frequency-locked sources such as the Agilent E4438 have random phase variation.

At a threshold power level, P_t, during the power sweep, the port wave signals are switched from the receivers of the VNA to the inputs of the sampling oscilloscope. Then the nose-to-nose-calibrated sampling oscilloscope is used to synchronously measure all spectral components on a frequency grid determined by the sampling rate and sampling duration. At P_t the absolute phases of the spectral components are available from the (phase-calibrated) oscilloscope-based measurements. Since the spectral components are also measured by the VNA at P_t, an absolute phase calibration becomes available for the signals measured by the VNA.

2.1 Calibration

Calibration of the NVNA requires the establishment of calibrated reference planes AA and BB in Fig. 1*a*. Full calibration requires linear (or relative) calibration, power calibration and absolute phase calibration. The calibration between the actual measurement planes and the ideal measurement planes, uses an eight-term linear error model [1]

$$\begin{bmatrix} a_1(f) \\ b_1(f) \\ a_2(f) \\ b_2(f) \end{bmatrix} = K(f) \begin{bmatrix} 1 & e_{12}(f) & 0 & 0 \\ e_{21}(f) & e_{22}(f) & 0 & 0 \\ 0 & 0 & e_{33}(f) & e_{34}(f) \\ 0 & 0 & e_{43}(f) & e_{44}(f) \end{bmatrix} \times \begin{bmatrix} A(f) \\ B(f) \\ C(f) \\ D(f) \end{bmatrix} \quad (1)$$

where the port waves at the DUT planes are denoted as a_1, b_1, a_2 and b_2, and the raw receiver measurements are denoted A, B, C and D. In the creation of an error model for a VNA, the actual receiver measurements and the port waves at the ideal measurement planes are assumed to be linearly related. Thus, at each frequency, a matrix containing error terms $e_{ij}(f)$ relates the actual receiver measurements and the port waves at the ideal measurement planes. For absolute phase calibration of a NVNA, an additional factor $K(f)$ is added to the error model to correct the absolute power and phase. In (1), the seven e's provide linear (or relative) calibration the magnitude of K provides power calibration and the phase of K provides phase calibration. This error model is determined at each IM frequency of interest. Each term of the error model is a complex number and in particular the error term $K(f)$ equals $|K(f)|e^{j\theta_K(f)}$.

Linear calibration determines the seven e's in the 4×4 matrix in (1) using a modified version of one of many procedures developed for linear VNAs [1, 4]. In linear calibration measurement, the hybrid NVNA connection in Fig. 1*a* is altered by replacing the DUT with calibration standards, replacing the two-tone source with a one-tone source and disregarding the reference receiver (R) measurements. The seven e's are then computed from the calibration measurements using known procedures. After linear correction to the DUT plane using the linear error model, only the relative power and phase between the port waves at each frequency have the correct values. (The relative nature of this calibration is indicated by the leading 1 in the matrix.) For absolute calibration, one of the port waves must be corrected in absolute power and phase, so that the other port waves can be corrected accordingly.

For broadband receiver-based NVNAs such as the sub-sampling mixer-based NVNA in [1], determining the terms in (1) provides complete calibration. Analytical descriptions of absolute power calibration that determines $|K(f)|$ using a power meter, and absolute phase calibration that determines $\theta_K(f)$ using a phase transfer standard, while accounting for the effects of mismatch, are given in [1]. In determining $\theta_K(f)$, which accounts for errors because of receiver phase dispersion, a multi-harmonic generator output is characterised using two of the receivers at port 1.

However, for narrowband receiver-based NVNAs such as the four-port VNA-based NVNA in [2], absolute phase calibration requires additional correction steps besides determining the terms in (1). Here the phase difference between the reference receiver R measurements and the DUT response (measured by receivers A–D), is added to the pre-determined phase value of the multi-harmonic generator to obtain the absolute phase of the port waves.

For the hybrid NVNA, the linear and power calibration procedures are the same for the oscilloscope- and heterodyne-based measurements. However, the two types of measurements require different absolute phase calibration procedures. Oscilloscope-based measurements are calibrated in absolute phase using the procedure described in [1] and used here. The absolute phase calibration procedure used here for heterodyne-based measurements differs from that in [2] and is described below.

2.1.1 Outline: The calibration procedure is made up of the calibration measurement part and the error correction part. The outline of the calibration measurement is as follows:

1. Establish the linear error model (see (1)).
2. Establish the power error $|K(f)|$.
3. Establish the phase error $\theta_K(f)$. $\theta_K(f)$ is the relative phase difference at each frequency f, between the reference receiver (R) used to measure the reference signal generator and each of the other receivers (A–D) used to measure the DUT signals at the DUT plane.

Just as for the four-port VNA-based NVNA, the heterodyne-based measurements use the reference receiver

© The Institution of Engineering and Technology 2011
IET Microw. Antennas Propag., 2011, Vol. 5, Iss. 5, pp. 616–624
doi: 10.1049/iet-map.2010.0580

(R) as a phase transfer mechanism between the sequentially sampled spectral components. As such, the relative phase error of the phase transfer mechanism as represented by $\theta_K(f)$ must be determined. This calibration step was not described in [2], but is obviously necessary since the reference receiver and the other receivers in a VNA give different measurements for the same signal. For this phase calibration measurement, the VNA portion of the hybrid NVNA is connected as in Fig. 1*b*. The output of the one-tone source is concurrently measured in receiver R and receivers A and B connected at the DUT plane AA at each IM frequency of interest. The load in the figure represents the off-state output impedance presented by the two-tone source with its RF output disabled. The analytical determination of $\theta_K(f)$ from the phase calibration measurements will be presented later.

After determining the errors from calibration measurements, the DUT measurements are corrected as follows:

1. Linear correction to the DUT plane using the linear error model.
2. Absolute power correction at the DUT planes using $|K(f)|$.
3. Absolute phase correction at the DUT planes uses $\theta_K(f)$, with the phase difference established over a power sweep between the concurrently measured reference signal generator and the DUT signals at the DUT plane, and with the phase of the DUT signals characterised at a specific power level by the sampling oscilloscope portion.

For the four-port VNA-based NVNA and the hybrid NVNA, $\theta_K(f)$ only corrects the relative phase error of the phase transfer mechanism, and so additional phase correction steps are required. For the hybrid NVNA, this is the third correction step above. In the following, descriptions are given first for the calibration step to determine $\theta_K(f)$, then for the absolute phase correction applied to the DUT measurements.

2.1.2 Phase calibration measurement: Connecting the one-tone source as in Fig. 1*b*, the port waves at the DUT plane AA must satisfy

$$M_{\mathrm{SigGen}}(f) = b_1(f) - \Gamma_{\mathrm{SigGen}}(f)a_1(f) \tag{2}$$

where M_{SigGen} is the output of the one-tone source, b_1 and a_1 are related to the VNA A and B receiver measurements from (1), and Γ_{SigGen} is its reflection coefficient characterised at the DUT plane AA using a VNA. Making the appropriate substitutions, (2) becomes

$$\begin{aligned} M_{\mathrm{SigGen}}(f) = {} & K(f)[e_{21}(f)A(f) + e_{22}(f)B(f)] \\ & - \Gamma_{\mathrm{SigGen}}(f)K(f)[A(f) + e_{12}(f)B(f)] \end{aligned} \tag{3}$$

Then solving for $K(f)$

$$K(f) = \frac{M_{\mathrm{SigGen}}(f)}{\begin{array}{c}[e_{21}(f)A(f) + e_{22}(f)B(f)] \\ -\Gamma_{\mathrm{SigGen}}(f)[A(f) + e_{12}(f)B(f)]\end{array}} \tag{4}$$

which has an angle $\theta_K(f)$. Since the relative phase error of the phase transfer mechanism is to be determined, the measured phase of receiver R is taken as the phase of M_{SigGen}. Noting that A and B are linearly related to M_{SigGen}, (4) implies that $\theta_K(f)$ is the relative phase difference between the measurement at receiver R and the mismatch corrected b_1. The power of M_{SigGen} has not been specified because it is not necessary in determining $\theta_K(f)$.

2.1.3 Phase correction of DUT measurements: In the following discussion, DUT characterisation is performed using a two-tone signal having frequencies f_1 and f_2, and so the incident excitation a_1 at f_1 and f_2 is considered. Also given a set of IM frequencies of interest, an arbitrary DUT port wave x at f_{IM} is considered.

For the VNA measurement, the responses at f_1, f_2 and f_{IM} are sequentially measured at time instants t_{f_1}, t_{f_2} and $t_{f_{\mathrm{IM}}}$, respectively. After correction, see (1), the phase of the sampled waveforms at the DUT plane is

$$\Phi_{a_1}(f_1, t_{f_1}, P_{\mathrm{in}}) = 2\pi f_1 t_{f_1} + \phi(f_1, t_{\mathrm{D}}) + \varphi(f_1, P_{\mathrm{in}}) \tag{5}$$

$$\Phi_{a_1}(f_2, t_{f_2}, P_{\mathrm{in}}) = 2\pi f_2 t_{f_2} + \phi(f_2, t_{\mathrm{D}}) + \varphi(f_2, P_{\mathrm{in}}) \tag{6}$$

$$\Phi_x(f_{\mathrm{IM}}, t_{f_{\mathrm{IM}}}, P_{\mathrm{in}}) = 2\pi f_{\mathrm{IM}} t_{f_{\mathrm{IM}}} + \phi(f_{\mathrm{IM}}, t_{\mathrm{D}}, P_{\mathrm{in}}) \tag{7}$$

where $\phi(f_1, t_{\mathrm{D}})$ and $\phi(f_2, t_{\mathrm{D}})$ are the particular startup phases of the two-tone sources. When setting the frequencies of the two-tone sources for a particular tone spacing, the two sources phase-lock at a particular relative phase that is held during the sequential power-swept measurements of all IM products. This phase profile changes if the frequencies of the two-tone sources are reset, and this effect is captured by the experiment time dependence t_{D}. During a power sweep, the switching attenuators in the two-tone sources also contribute phase shifts $\varphi(f_1, P_{\mathrm{in}})$ and $\varphi(f_2, P_{\mathrm{in}})$ that are time independent but vary with the power P_{in} of the two-tone signal. The term $\phi(f_{\mathrm{IM}}, t_{\mathrm{D}}, P_{\mathrm{in}})$ in (7) is the phase of the DUT response. Since the DUT response depends on the incident excitation, $\phi(f_{\mathrm{IM}}, t_{\mathrm{D}}, P_{\mathrm{in}})$ will depend both on t_{D} and P_{in}.

The reference signal generator output is concurrently sampled by the reference receiver R at the same measurement times t_{f_1}, t_{f_2} and $t_{f_{\mathrm{IM}}}$ as the measurements described by (5)–(7). The phase values are

$$\Psi_{\mathrm{R}}(f_1, t_{f_1}) = 2\pi f_1 t_{f_1} + \psi(f_1, t_{f_1}) \tag{8}$$

$$\Psi_{\mathrm{R}}(f_2, t_{f_2}) = 2\pi f_2 t_{f_2} + \psi(f_2, t_{f_2}) \tag{9}$$

$$\Psi_{\mathrm{R}}(f_{\mathrm{IM}}, t_{f_{\mathrm{IM}}}) = 2\pi f_{\mathrm{IM}} t_{f_{\mathrm{IM}}} + \psi(f_{\mathrm{IM}}, t_{f_{\mathrm{IM}}}) \tag{10}$$

where ψ indicates the startup phase of the reference signal generator each time it is tuned to a different measurement frequency. Note that in (8)–(10) there is no dependence on P_{in} since the reference signal generator maintains a constant output power and thus the same relative phase during a power sweep.

The phase correction procedure can now be described. First, the phase is corrected relative to the reference receiver as follows

$$\begin{aligned} \Phi'_{a_1}(f_1, t_{f_1}, P_{\mathrm{in}}) &= \Phi_{a_1}(f_1, t_{f_1}, P_{\mathrm{in}}) - \Psi_{\mathrm{R}}(f_1, t_{f_1}) \\ &= \phi(f_1, t_{\mathrm{D}}) + \varphi(f_1, P_{\mathrm{in}}) - \psi(f_1, t_{f_1}) \end{aligned} \tag{11}$$

© The Institution of Engineering and Technology 2011

$$\Phi'_{a_1}(f_2, t_{f_2}, P_{\text{in}}) = \Phi_{a_1}(f_2, t_{f_2}, P_{\text{in}}) - \Psi_{\text{R}}(f_2, t_{f_2}) = \phi(f_2, t_{\text{D}}) + \varphi(f_2, P_{\text{in}}) - \psi(f_2, t_{f_2}) \tag{12}$$

$$\Phi'_x(f_{\text{IM}}, t_{f_{\text{IM}}}, P_{\text{in}}) = \Phi_x(f_{\text{IM}}, t_{f_{\text{IM}}}, P_{\text{in}}) - \Psi_{\text{R}}(f_{\text{IM}}, t_{f_{\text{IM}}}) = \phi(f_{\text{IM}}, t_{\text{D}}, P_{\text{in}}) - \psi(f_{\text{IM}}, t_{f_{\text{IM}}}) \tag{13}$$

At this stage, for each spectral component, the relative phases of measurements at different powers in a power sweep are established. However, the phase relationship of different spectral components is arbitrary, since the phase of the reference signal generator varies as it is tuned to different measurement frequencies. The next step in the phase correction procedure is to determine an absolute phase reference.

The key is to cross-reference the corrected phase from the VNA-based data, for example, (11)–(13), with the absolute phase derived from measurements made with the sampling oscilloscope. The oscilloscope-based measurements at a chosen excitation power P_{t} provide the needed absolute phase reference. All spectral components are captured by the oscilloscope at the same time, t_{DSO}. The relative phase profile of the two-tone sources is set at experiment time t_{D}. For the same incident excitation frequency and power level, the DUT response will be the same and the absolute phase values corrected to the DUT plane are

$$\Phi_{a_1,\text{DSO}}(f_1, t_{\text{DSO}}, P_{\text{t}}) = 2\pi f_1 t_{\text{DSO}} + \phi(f_1, t_{\text{D}}) + \varphi(f_1, P_{\text{t}}) \tag{14}$$

$$\Phi_{a_1,\text{DSO}}(f_2, t_{\text{DSO}}, P_{\text{t}}) = 2\pi f_2 t_{\text{DSO}} + \phi(f_2, t_{\text{D}}) + \varphi(f_2, P_{\text{t}}) \tag{15}$$

$$\Phi_{x,\text{DSO}}(f_{\text{IM}}, t_{\text{DSO}}, P_{\text{t}}) = 2\pi f_{\text{IM}} t_{\text{DSO}} + \phi(f_{\text{IM}}, t_{\text{D}}, P_{\text{t}}) \tag{16}$$

which are repeatable to within an unknown phase $2\pi f_{\text{IM}} t_{\text{DSO}}$ at each IM frequency.

The final phase correction step makes use of the absolute phase reference established by the oscilloscope measurements to relate the phase of different spectral components measured by the VNA. The phase values, (11)–(13), measured by the VNA over a power sweep, are shifted to the absolute phase (14)–(16) measured by the oscilloscope at power level P_{t}, as follows

$$\Phi''_{a_1}(f_1, t_{\text{DSO}}, P_{\text{in}}) = \Phi_{a_1,\text{DSO}}(f_1, t_{\text{DSO}}, P_{\text{t}}) + (\Phi'_{a_1}(f_1, t_{f_1}, P_{\text{in}}) - \Phi'_{a_1}(f_1, t_{f_1}, P_{\text{t}})) = 2\pi f_1 t_{\text{DSO}} + \phi(f_1, t_{\text{D}}) + \varphi(f_1, P_{\text{in}}) \tag{17}$$

$$\Phi''_{a_1}(f_2, t_{\text{DSO}}, P_{\text{in}}) = \Phi_{a_1,\text{DSO}}(f_2, t_{\text{DSO}}, P_{\text{t}}) + (\Phi'_{a_1}(f_2, t_{f_2}, P_{\text{in}}) - \Phi'_{a_1}(f_2, t_{f_2}, P_{\text{t}})) = 2\pi f_2 t_{\text{DSO}} + \phi(f_2, t_{\text{D}}) + \varphi(f_2, P_{\text{in}}) \tag{18}$$

$$\Phi''_x(f_{\text{IM}}, t_{\text{DSO}}, P_{\text{in}}) = \Phi_{x,\text{DSO}}(f_{\text{IM}}, t_{\text{DSO}}, P_{\text{t}}) + (\Phi'_x(f_{\text{IM}}, t_{f_{\text{IM}}}, P_{\text{in}}) - \Phi'_x(f_{\text{IM}}, t_{f_{\text{IM}}}, P_{\text{t}})) = 2\pi f_{\text{IM}} t_{\text{DSO}} + \phi(f_{\text{IM}}, t_{\text{D}}, P_{\text{in}}) \tag{19}$$

These are the so-called absolute phase measurements because receiver and interconnect phase dispersion across a broad range of spectral components being measured have been corrected.

Note that (17)–(19) are repeatable to within an unknown phase $2\pi f_{\text{IM}} t_{\text{DSO}}$ at each IM frequency. This is because phase is intrinsically a relative quantity that depends on the sampling time. Even during the characterisation of a phase transfer standard, different phase values are measured at different times. For example, even though a multi-harmonic generator is designed to maintain a constant phase relationship among the spectral components, it has a time-varying phase at its fundamental component. Phase locking the signal source and the receivers cannot solve the problem because of the imperfect phase-locking mechanism that exhibits long-term drift and because of the unknown initial relative phase established by the phase lock.

Absolute phase measurement also requires the ability to compare measurements made at different times. The solution is to measure the incident excitation simultaneously with the DUT response. Then to compare measurements made at different times, the different sets of data are shifted to a common time origin using an alignment procedure [5], which removes the arbitrary time delays between the data sets. Assuming that one set of measurements is a time-delayed version of the other, the time delay between the incident excitations can be found, and all scattered port waves are adjusted by this time delay. This requires that the incident excitations be of the same type, such as two-tone signals with the same tone spacing, amplitude and phase profile.

The other solution is to apply the time-invariant phase definition [5] to find the phase relation between the incident excitation and the scattered port waves. This yields more intuitive results in typical DUT non-linear characterisation since the engineer is interested in the phase change caused by the DUT as a function of input power or tone spacing. However, as discussed in [5], the alignment procedure is more robust (than the time-invariant procedure) from noise considerations. This restricts the application of the time-invariant phase definition to narrow-band signals such as two-tones or weakly non-linear characterisation for wideband signals such as multi-tones. Nevertheless, the intuitive results of time-invariant phase definition is invaluable in design, since measurements of different tone spacings can be compared and the phase contributions from the switching attenuator in the signal generator can also be removed. Strictly speaking, these phase contributions are part of the signal being characterised. So, absolute phase measurement using the alignment procedure is best suited to signal characterisation. In the following, it will be shown that the time-invariant phase definition yields only the phase change caused by the DUT, and thus more suitable for DUT characterisation.

2.2 Input–output phase relation

In the following discussion, the DUT is represented as a Volterra series for simplicity. For a two-tone excitation, the

© The Institution of Engineering and Technology 2011
IET Microw. Antennas Propag., 2011, Vol. 5, Iss. 5, pp. 616–624
doi: 10.1049/iet-map.2010.0580

response at f_{IM} is

$$Y(f_{\mathrm{IM}}) = \sum_{n} \sum_{\boldsymbol{m}_{n,\mathrm{IM}}} \frac{(n{:}\boldsymbol{m})}{2^n} (A_2^*)^{m_{-2}} (A_1^*)^{m_{-1}} (A_1)^{m_1} (A_2)^{m_2} \times H_n(f_{-2(1)}, \ldots, f_{-2(m_{-2})}, f_{-1(1)}, \ldots, f_{-1(m_{-1})}, f_{1(1)}, \ldots, f_{1(m_1)}, f_{2(1)}, \ldots, f_{2(m_2)}) \quad (20)$$

where H_n denotes the nth-order Volterra non-linear transfer function (NLTF), $\boldsymbol{m}_{n,\mathrm{IM}}$ denotes the nth-order contributing mixing vectors and A denotes the complex amplitude of the excitation tones. Using the shortened notation $H_n(\boldsymbol{m})$ to denote H_n evaluated at the mixing product corresponding to $\boldsymbol{m}$, (20) can be rearranged as

$$\begin{aligned} Y(f_{\mathrm{IM}}) &= \sum_{n} \sum_{\boldsymbol{m}_{n,\mathrm{IM}}} \frac{(n{:}\boldsymbol{m})}{2^n} |A_2|^{m_{-2}} |A_1|^{m_{-1}} |A_1|^{m_1} |A_2|^{m_2} |H_n(\boldsymbol{m})| \\ &\quad \times \mathrm{e}^{\mathrm{j}(\theta_{A_1}(m_1-m_{-1})+\theta_{A_2}(m_2-m_{-2})+\theta_{H_n(\boldsymbol{m})})} \\ &= \mathrm{e}^{\mathrm{j}(\theta_{A_1}(m_1-m_{-1})+\theta_{A_2}(m_2-m_{-2}))} \\ &\quad \times \left[\sum_{n} \sum_{\boldsymbol{m}_{n,\mathrm{IM}}} \frac{(n{:}\boldsymbol{m})}{2^n} |A_2|^{m_{-2}} |A_1|^{m_{-1}} \right. \\ &\quad \left. \times |A_1|^{m_1} |A_2|^{m_2} |H_n(\boldsymbol{m})| \mathrm{e}^{\mathrm{j}\theta_{H_n(\boldsymbol{m})}} \right] \\ &= \mathrm{e}^{\mathrm{j}(\theta_{A_1}(m_1-m_{-1})+\theta_{A_2}(m_2-m_{-2}))} [|Y(f_{\mathrm{IM}})| \mathrm{e}^{\mathrm{j}\theta_{\mathrm{DUT}}(|A_1|,|A_2|,H)}] \end{aligned} \quad (21)$$

The second step is possible because each component of the double sum contributes to the same $f_{\mathrm{IM}} = (m_1 - m_{-1})f_1 + (m_2 - m_{-2})f_2$. In the last step, the double sum is rewritten as a complex number with the phase $\theta_{\mathrm{DUT}}(|A_1|, |A_2|, H)$ depending only on the excitation magnitude and the DUT NLTF.

Applying the time-zero cancellation definition [5], the time-invariant phase is

$$\begin{aligned} \phi'_{f_{\mathrm{IM}}} &= \phi_{f_{\mathrm{IM}}} - (\theta_{A_1}(m_1 - m_{-1}) + \theta_{A_2}(m_2 - m_{-2})) \\ &= \theta_{\mathrm{DUT}}(|A_1|, |A_2|, H) \end{aligned} \quad (22)$$

In application to the current measurement, the switching attenuator contributions $\varphi(f_1, P_{\mathrm{in}})$ and $\varphi(f_2, P_{\mathrm{in}})$ to the excitation tone phase θ_{A_1} and θ_{A_2}, respectively, will be cancelled.

3 Measurement

The hybrid NVNA is applied to the non-linear characterisation of a power amplifier using a two-tone signal with frequencies f_1 and f_2 centred at $(f_1 + f_2)/2 = 2$ GHz with a $(f_2 - f_1) = 200$ kHz tone spacing. The power amplifier is an Amplica SD513301 with approximately 20 dB gain between 900 MHz and 2 GHz, and 17 dBm output at the 1 dB compression point. The procedure for correcting the raw DUT measurements is illustrated here by plotting the port waves during a power sweep after each correction step. For simplicity only results at the lower fundamental frequency f_1 and lower IM3 frequency $2f_1 - f_2$ are presented.

Figs. 2 and 3 present the amplitudes and phases of power waves following the correction described in (1) that includes linear correction, power correction and relative phase error correction. Fig. 2*a* shows that at the lower fundamental frequency f_1, the incident wave at port 1, $a_1(f_1)$, is linearly increased during the power sweep. Also at the same frequency, the power of the transmission wave at port 2, b_2, undergoes compression, while the reflected wave at port 1, b_1, undergoes expansion. Since b_2 is reflected by an imperfect load, there is an incident wave at port 2, a_2, which also shows compression. At the lower IM3 frequency $2f_1 - f_2$, there is no incident wave at port 1. At the same frequency, Fig. 3*a* shows that the power of the transmission wave b_2 undergoes compression, while the reflected wave at port 1, b_1, undergoes a null presumably because of cancellation by lower-order and higher-order contributions. Owing to reflection by an imperfect load, there is also an incident wave a_2 that also shows compression. Both Figs. 2*b* and 3*b* show that the phases of the port waves track each other during the power sweep, indicating that the VNA receivers are synchronous.

Only the relative phase error of the phase transfer mechanism has been corrected so far, and so additional

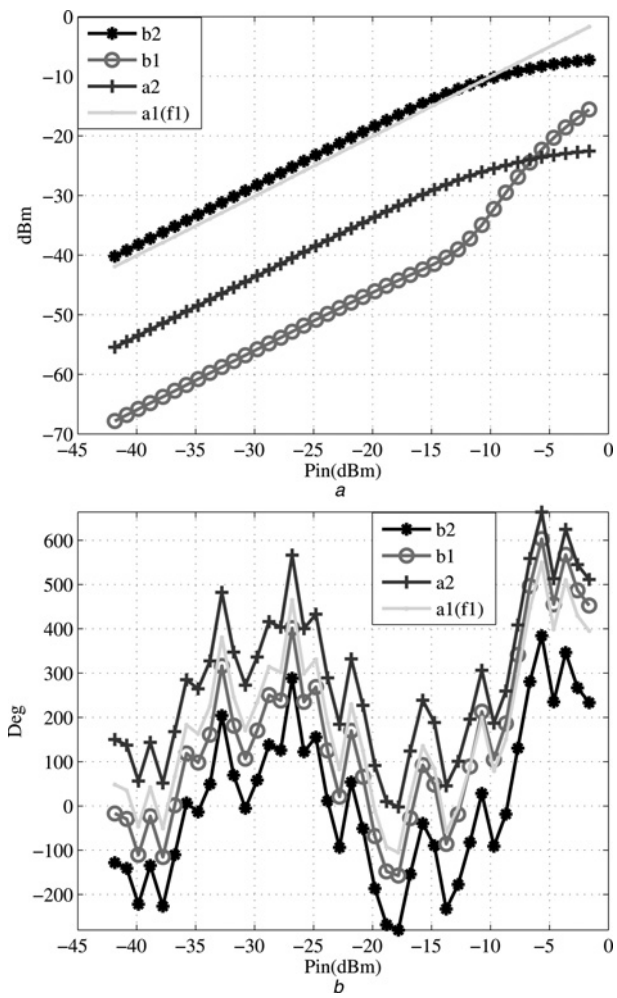

Fig. 2 *Power waves at the fundamental frequency f_1 for a two-tone test at 2 GHz with 200 kHz tone spacing following the first phase correction described in (1)*

a Amplitude
b Phase

© The Institution of Engineering and Technology 2011

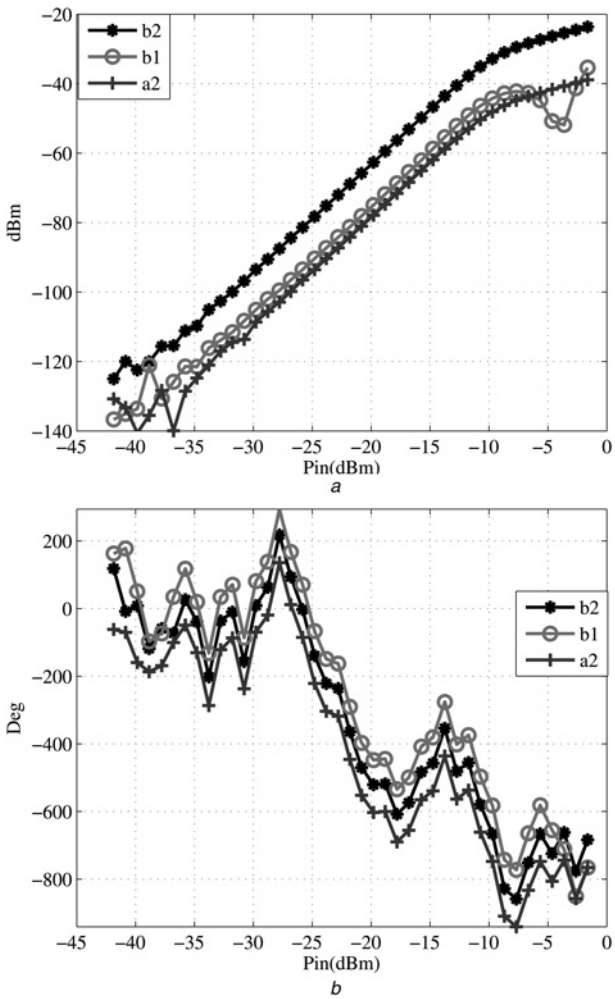

Fig. 3 *Power waves at the IM3 frequency $2f_1 - f_2$ for a two-tone test at 2 GHz with 200 kHz tone spacing following the first phase correction described in (1)*

a Amplitude
b Phase

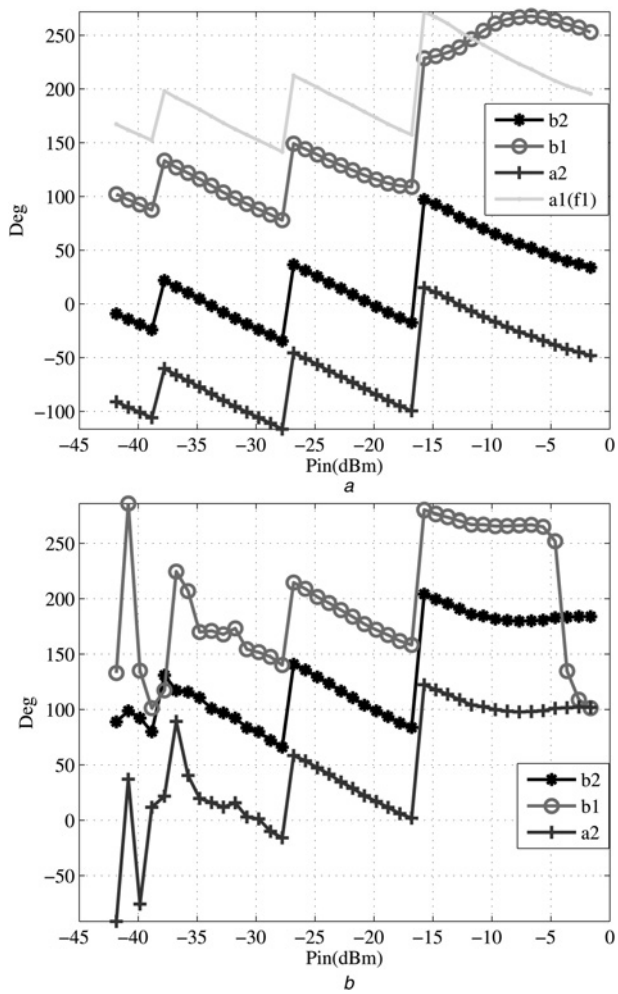

Fig. 4 *Phases of power waves at ports 1 and 2 for the two-tone test following the final phase correction step as described in (17)–(19)*

a At the fundamental, f_1
b At the IM3, $2f_1 - f_2$

phase correction steps are required. The remaining steps correct for the phase measurement and have no effect on the amplitude characterisation. In the second correction step described by (11)–(13), the phase of the reference signal generator (which is constant during a power sweep), is subtracted from the VNA measurements corrected in the first correction step. In the final correction step described in (17)–(19), the power sweep data are shifted to the absolute phase reference provided by the oscilloscope-based measurements at a chosen excitation power. After these correction steps, Fig. 4 shows the phases of power waves. This result is an absolute phase measurement since the receiver phase dispersion has been removed.

At this point, the alignment procedure can be applied to compare different sets of data. Even with alignment, which simply shifts each curve in Figs. 4*a* and *b* up or down by a constant phase value, there will still be abrupt phase jumps. The phase jumps are because of the switching attenuator in the two-tone sources and this dependency shows up in (17)–(19) as the dependence on P_{in}. Strictly speaking, these phase jumps are part of the signal being characterised. So absolute phase measurement using the alignment procedure is best suited to signal characterisation.

More intuitively satisfying DUT characterisation results are obtained by applying the time-invariant phase definition described by (22). Fig. 5 shows that the phase contribution of the multi-tone signal generators is removed, and the scattered port waves have a slowly varying phase change that is only contributed to by the DUT. For the lower fundamental frequency f_1 in Fig. 5*a*, the phase of the port 1 reflected wave, b_1, undergoes expansion, which correlates with the magnitude expansion observed in Fig. 2*a*. For the lower IM3 frequency $2f_1 - f_2$ in Fig. 5*b*, the port 1 reflected wave b_1 undergoes abrupt phase change at high input power levels, which correlates with the IM3 sweet-spot observed in the magnitude response in Fig. 3*a*.

4 Discussion

4.1 Assumptions

The phase-locked signal generator must meet several requirements for the proposed approach to work. Firstly, stable phase lock is needed for the power sweep for each spectral component. This is easily met as the Marconi 2024 can provide hours of stable phase lock and has been successfully used in a high dynamic range feed-forward cancellation system [6, 7].

© The Institution of Engineering and Technology 2011
IET Microw. Antennas Propag., 2011, Vol. 5, Iss. 5, pp. 616–624
doi: 10.1049/iet-map.2010.0580

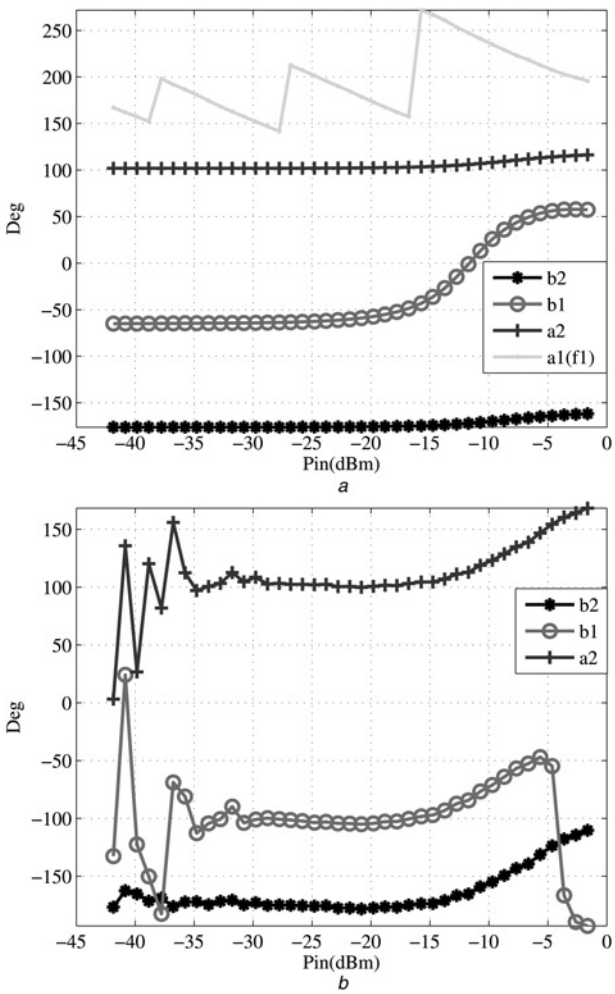

Fig. 5 *Phases of power waves for the two-tone test after applying the time-invariant phase definition (22)*

a At the fundamental, f_1
b At the IM3, $2f_1 - f_2$

Secondly, the power output of the multi-tone source must be repeatable during the power sweep to provide a repeatable test signal. This has been empirically verified. Since the phase reference signal generator is set to constant output power this is not an issue.

Most importantly, stable phase-lock is also needed during the time interval in which all of the spectral components are measured by the VNA and oscilloscope portions of the hybrid NVNA. This is so that the multi-tone sources are locked in phase, and provide repeatable input for the power sweep at all spectral components. For example, if power is swept over 30 dB with 1 dB resolution and each point takes 1 s in the VNA, then each spectral component takes 30 s. For two-tone testing measuring all fifth-order responses, the 30 spectral components will take 15 min. So the hours of stable phase-lock time available is sufficient including the oscilloscope acquisition time. For sweeps over tone-spacing, the input frequency changes and the phase lock is lost in any case, and complete phase recalibration is (automatically) required.

4.2 Measurement time

In measurements at a particular tone spacing using the hybrid NVNA, the VNA portion acquires data at all spectral components with swept excitation power levels and the oscilloscope portion acquires data at all spectral components at one power level. Compared to the previously reported four-port VNA-based NVNA, the hybrid NVNA requires additional data acquisition from its oscilloscope portion. If the hybrid NVNA uses an outdated sampling oscilloscope, the duration of each oscilloscope acquisition is dominated by the data transfer time over the GPIB interface. At each tone spacing, the acquisition duration of the oscilloscope portion is comparable to the acquisition duration of the VNA portion. In this case, the hybrid NVNA doubles the measurement time when compared with that of the four-port VNA-based NVNA. If the hybrid NVNA uses a sampling oscilloscope with a faster data transfer interface, then the duration of each oscilloscope acquisition is negligible when compared with the duration of the VNA acquisition. In this case, the hybrid NVNA takes approximately the same amount of measurement time as the four-port VNA-based NVNA.

In the sub-sampling mixer-based NVNA measurement at a particular tone spacing, all spectral components at each power level are captured at once. At each power level, the total data acquisition time is approximately the same as the amount of time it takes the VNA to capture one spectral component. Thus, the hybrid NVNA measurement time exceeds the sub-sampling mixer-based NVNA measurement time by a factor equaling the number of spectral components being measured.

4.3 Tone-spacing limitations

Now that the phase reference signal generator can be fine tuned in 1 Hz steps (typically), the minimum tone spacing is established by other issues related to measuring a weak tone next to a strong tone. First, the heterodyne receivers of the VNA is FFT-based. So when two tones are present in the signal, the rectangular window used in the FFTs creates spectral leakage that only decays at 6 dB per octave. Although the VNA has a minimum resolution bandwidth of 1 Hz, the weak tone needs to be 100 s of hertz away from the strong tone to be measured with about 50 dB dynamic range.

Secondly, the phase noise of the multi-tone sources can degrade the accuracy of the measured IM product. Using the Marconi 2024 to generate a two-tone signal with 200 Hz tone spacing, this effect noticeably affects the accuracy for IM3 product 45 dBc down as shown in Fig. 6.

The last issue is that the memory depth of the oscilloscope may be too small for the desired frequency resolution. For an RF frequency of 1 GHz, tone spacing of 1 kHz and Nyquist sampling upto the first harmonic band, two mega-samples are needed. This is readily available.

4.4 Dynamic range

The dynamic range of the hybrid NVNA can determined either from the amplitude or the phase response. In the following discussion, the transmission wave at port 2, b_2, is considered because it has the highest IM ratio (in dBc) and is the most difficult to measure. For measurements with tone-spacing set at 200 kHz, Fig. 3*a* is the amplitude response at the lower IM3 frequency as the two-tone signal ramps from low power to high power with the power of each tone being equal. At low two-tone powers it is expected that the response level (in dBm) will vary linearly with changes in the two-tone power. Thus, a departure from linearity indicates the minimum detectable signal, which here is −122 dBm with corresponding P_{in} of −40 dBm. At

© The Institution of Engineering and Technology 2011

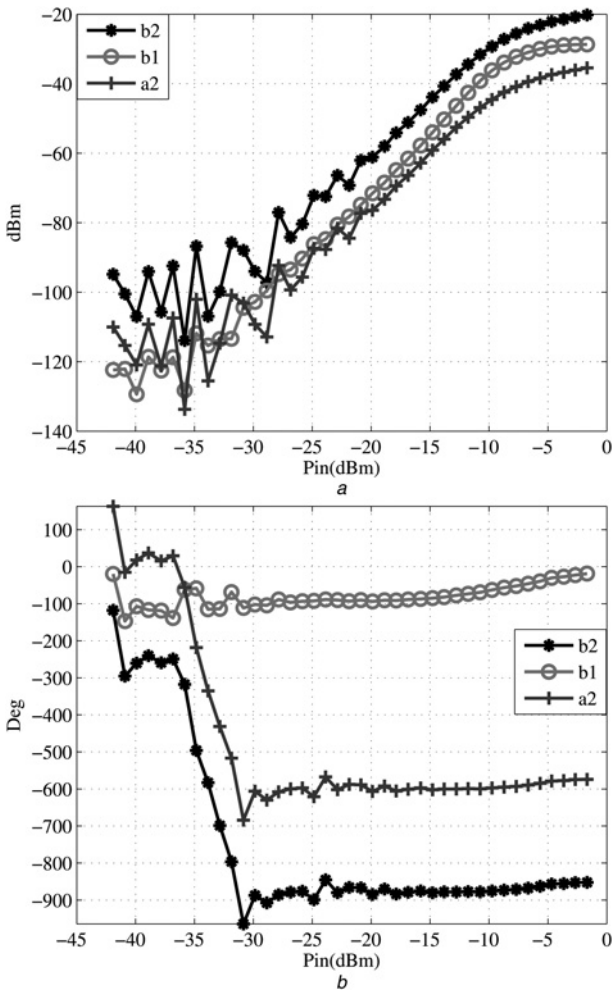

Fig. 6 *Power waves at the IM3 frequency $2f_1 - f_2$ for a two-tone test at 2 GHz with 200 Hz tone spacing after applying the time-invariant phase definition (22)*

a Amplitude
b Phase

the same P_{in} in Fig. 2*a*, the lower fundamental is −39 dBm. This indicates that the dynamic range is 83 dB. Similarly, for a two-tone signal with tone spacing set at 200 Hz, Fig. 6*a* shows that the minimum detectable signal is −62 dBm with corresponding P_{in} of −21 dBm. At the same P_{in}, the lower fundamental is −20 dBm, which indicates that the dynamic range is 42 dB.

The phase response is more sensitive to noise, and more accurate in determining the minimum detectable signal. At low two-tone powers, it is expected that the phase of the response will stay constant with changes in the two-tone power; thus, a departure from a constant phase indicates the minimum detectable signal. For a two-tone signal with tone spacing set at 200 kHz, Fig. 5*b* shows that the minimum detectable signal corresponds to a P_{in} of −37 dBm. From the corresponding power level in Fig. 2*a* for the lower fundamental and Fig. 3*a* for the lower IM3, which are −116 and −35 dBm, respectively, the dynamic range is computed to be 79 dB. For a two-tone signal with tone spacing set at 200 Hz, Fig. 6*b* shows that the minimum detectable signal corresponds to a P_{in} of −20 dBm. Similarly, from the corresponding power level for the lower fundamental and the lower IM3, the dynamic range is computed to be 40 dB.

The usable dynamic range of the hybrid NVNA is about 40 dB at 200 Hz tone spacing and this monotonically increases to about 80 dB at 200 kHz tone spacing. While this is an improvement over the previously reported four-port VNA-based NVNA, the dynamic range is still well below what is required to measure heating effects in planar transmission lines [7]. What can be characterised are the long-term memory effects in RF amplifier circuits, where third-order IM products of concern are typically at the −40 dBc level. The fifth- and seventh-order contributions to the IM products are typically present at about the −20 dBc level and can also be measured. At narrow tone spacings, the limitation in dynamic range is due in large part to the phase noise in the phase-locked sources that are combined as the multi-tone excitation. In the feedforward cancellation system presented in [7], along with the discrete tone, the phase noise can also be cancelled since the phase noise of one source is phase synchronous with the phase noise of the other. In the hybrid NVNA, the discrete tones are measured rather than being cancelled and the SNR is degraded by the phase noise.

5 Conclusion

A wideband hybrid NVNA was presented that combines high dynamic range with very low-frequency separation of tones in a two-tone test. The hybrid NVNA can be implemented using instruments generally available in a microwave laboratory: phase-locked signal generators, a four-port VNA and a sampling oscilloscope. Tone spacings as low as 1 Hz are supported. High dynamic range is obtained from the heterodyne system incorporated in the four-port VNA. The absolute phase reference required in non-linear vector network analysis is provided by a reference oscillator phase locked to each of the two sources providing the tones in a two-tone test. A sampling oscilloscope is used to complete the absolute phase calibration process. In effect the hybrid NVNA combines the high dynamic range of the heterodyne-based architecture with the arbitrary tone spacings that the oscilloscope-based system supports. Using each architecture to its advantage achieves narrow tone spacing, wide bandwidth and high dynamic range. The narrowest tone-spacing usable is now determined by the memory depth of the oscilloscope, the windowing effect of the heterodyne receivers and the phase noise of the multi-tone sources.

6 References

1 Verspecht, J.: 'Calibration of a measurement system for high frequency nonlinear devices'. PhD thesis, Vrije Universiteit Brussel, 1995
2 Blockley, P.S., Gunyan, D., Scott, J.B.: 'Mixer-based, vector-corrected, vector signal/network analyzer offering 300 kHz–20 GHz bandwidth and traceable phase response'. IEEE MTT-S Int. Microwave Symp. on Digest, June 2005, pp. 1497–1500
3 Williams, D.F., Clement, T.S., Remley, K.A., Hale, P.D., Verbeyst, F.: 'Systematic error of the nose-to-nose sampling-oscilloscope calibration', *IEEE Trans. Microw. Theory Tech.*, 2007, **55**, (9), pp. 1951–1957
4 Steer, M.B.: 'Microwave and RF design: a systems approach' (SciTech Publishing, Inc., Raleigh, NC, 2010)
5 Blockley, P.S., Scott, J.B., Gunyan, D., Parker, A.E.: 'Noise considerations when determining phase of large-signal microwave measurements', *IEEE Trans. Microw. Theory Tech.*, 2006, **54**, (8), pp. 3182–3190
6 Walker, A., Steer, M.B., Gard, K.G.: 'A vector intermodulation analyzer applied to behavioral modeling of nonlinear amplifiers with memory', *IEEE Trans. Microw. Theory Tech.*, 2006, **54**, (5), pp. 1991–1999
7 Wilkerson, J.R., Gard, K.G., Steer, M.B.: 'Automated broadband high-dynamic-range nonlinear distortion measurement system', *IEEE Trans. Microw. Theory Tech.*, 2010, **58**, (5), pp. 1273–1282

© The Institution of Engineering and Technology 2011

doi: 10.1049/iet-map.2010.0580